International Journal of the Physical Sciences Vol. 5 (2), pp. 132-144, February, 2010
Available online at http://www.academicjournals.org/IJPS
ISSN 1992 - 1950 © 2010 Academic Journals

Full Length Research Paper

Experimental and numerical analysis of end anchored steel plate and CFRP laminate flexurally strengthened reinforced concrete (r. c.) beams

Mohd Zamin Jumaat and M. D. Ashraful Alam*

Department of Civil Engineering, University of Malaya, 50603 Kuala Lumpur, Malaysia.

Accepted 22 January, 2010

End anchors have been shown to significantly reduce premature plate end debonding failure of plate bonded strengthened reinforced concrete (r. c.) beams. One of the main interest in designing end anchors is to determine the minimum or optimal length of end anchors for a given thickness and height of the end anchor. This paper presents experimental and numerical studies in determining those optimum lengths for steel plate and carbon fibre reinforced polymer (CFRP) laminate flexurally strengthened r. c. beams. In the experimental programme, seven r. c. beams were cast. One beam was tested in the un-strengthened condition to act as the control beam. Three beams were strengthened with steel plates and another three beams were strengthened with CFRP laminates. From each group of the strengthened beams, one beam was strengthened without any end anchor, one was end anchored using the optimum anchorage length and the last one was end anchored using an arbitrarily 200 mm anchorage length. The optimum length for the end anchor used in this study was derived from analyzing the interfacial stress diagram of the strengthened beams and was found to be approximately 100 mm. The beams were also modelled using FEM (LUSAS). The results indicate that the optimized 100 mm anchorage length plates were able to prevent premature plate end debonding failure of steel plate and CFRP laminate strengthened beams satisfactorily. It could also be seen from the results that beams with end anchors had a higher failure loads and had more ductile behaviour than the un-anchored strengthened beams. Results also show that the optimized end anchored strengthened beams had identical structural behaviour to that of the longer end anchored strengthened beams. The numerical results are able to predict the behaviour of the beams satisfactorily.

Key words: Premature debonding, end peeling, CFRP laminate, steel plate, end anchors.

INTRODUCTION

Strengthening of reinforced concrete structures is an important task in the field of structural maintenance. Reinforced concrete structures need to be strengthened for a number of reasons. These include the increase in loads as a result of functional changes of the structures, overloading, under-design of existing structures or the lack of quality control.

Different types of strengthening materials are available in the market for this purpose. These include ferro cement, sprayed concrete, steel plate and fibre reinforced polymer (FRP) laminate. Generally, the use of steel plate and FRP laminates, referred to as plate bonding, is preferred due to their advantages such as easy construction work, minimum change in the overall size of the structure and less disruption to traffic.

Plate bonding method of strengthening often suffers for premature debonding failure problems resulting from the separation of plates and concrete rip off along the tensile reinforcing bars before the full ultimate loads. These failures are normally brittle in nature. These debonding can be broadly classified into plate end debonding or end peeling, axial peeling and debonding at the interface level. Amongst these, plate end debonding failure is the most common (Smith and Teng, 2002).

The mechanism that causes plate end debonding failure has been investigated and reported by a number of researchers (Saadatmanesh and Malek, 1998; El-

*Corresponding author. E-mail: ashraf_arif2003@yahoo.com or ashraful@perdana.um.edu.my. Tel: +6-0163040495.

Mihilmy and Tedesco, 2001; Yao and Teng, 2007; Yang et al., 2008). In general it was concluded that high interfacial shear stresses concentration at the ends of the bonded plates were responsible for plate end debonding failure (Bahn et al., 2008). Thus, research to eliminate plate end debonding failure to obtain full strength of strengthened beams with the desired ductility is very crucial.

Various traditionally anchor bolts had been used to reduce debonding failure. This technique was found to be not very effective (Hussain et al., 1995; Garden, 1998; Jones et al., 1998 and Chahrour and Soudki, 2005). This is due to the fact that anchor bolts could only resist normal stress rather than shear stress of strengthening plates.

To overcome the limitations of anchor bolts, end anchors using U and L-shaped wrap and plates are the popular choice. These have been experimentally investigated by a number of researchers (Hosny et al., 2006; Ceroni et al., 2008; Bahn and Harichandran, 2008; Jumaat and Alam, 2008; Kim et al., 2008). Results of past researches showed that U and L-shaped end anchors significantly reduce premature plate end debonding failure (Jumaat and Alam, 2008; Bahn et al., 2008).

These researches, however, did not look into determining the most effective way of utilizing end anchors. The dimensions of the end anchors used were chosen arbitrarily. From the literature work carried out, there was a general conclusion that the development of an excessive interfacial shear stress at the plate end is the main reason to cause premature plate end debonding failure. Anchorage length of end anchors as a result of this finding could be obtained from the interface shear stress diagram of the strengthened beams.

Works on studying the structural behaviour of end anchored strengthened beams based on numerical analysis were also limited. The objectives of this study were to investigate the effectiveness of the optimum end anchor length approach experimentally and to show the results could also be achieved using a Finite element method (FEM) analysis.

EXPERIMENTAL INVESTIGATION

Description of specimens

Seven r. c. beams of rectangular cross-sections were tested in this study. The details of those beams are shown in Table 1. From the strengthened beams, beams B1 and C1 were end anchored using L-shaped anchor plates of 100 mm anchorage length, whereas beams B2 and C2 were end anchored using end anchors of 200 mm anchorage length. Beams B0 and C0 had no end anchors to study the effect of end anchors. An anchorage length of 100 mm was obtained from the interfacial shear stress diagram (Figure 3), whereas 200 mm was chosen arbitrarily. Both end anchors were used to prevent end peeling. The test variables are summarized in Table 1.

Fabrication of specimens

All beam specimens were 2300 mm long, 125 mm wide, and 250 mm deep as shown in Figure 1. These beams were reinforced with two 12 mm diameter steel bars in the tension zone as main reinforcement. Two 10 mm steel bars were used as hanger bars in the shear span and were placed at the top of each beam. Six mm bars were used for shear reinforcement and were symmetrically placed. The spacing of the shear reinforcement was 75 mm. The details of all reinforcements are shown in Figure 1.

Strengthening and anchoring

For all beams, the length of the bonded plate was 1900 mm, which covered almost the full-span length of the beams (Figure 2). To obtain a perfect bond, the concrete surface was ground with a diamond cutter to expose the coarse aggregates. Dust was then blown out using compressed air. The surface of the steel plate was sand blasted to eliminate rust.

Colma cleaner was used to remove carbon dust from the bonding face of the CFRP laminate. In this research, sikadur adhesive was used as a bonding agent. It has an excellent bonding strength. The components (resin and hardener) of this adhesive was mixed according to the guidelines of the manufacturer. Well mixed sikadur adhesive was then trawled on to the surface of the concrete specimens to form a thin layer. The adhesive was also applied with a special “dome” shaped spatula onto the CFRP (Sika CarbaDur) laminates and steel plates. The plates were positioned on the prepared surface. Using a rubber roller, the plates were gently pressed into the adhesive until the material was forced out on both sides of the laminates. The surplus adhesive was then removed.

L-shaped end anchors were placed at the ends of all strengthened beams. All anchors were made of steel plates of 2 mm thickness. The thickness of the plate was 2 mm. Anchorage lengths of 100 mm and 200 mm were used for end anchoring of steel plate and CFRP laminate strengthened beams. The interfacial shear stress diagram of strengthened beams which is the basis of optimal end anchors is shown in Figure 3. This interfacial shear stress diagram was obtained from the result of finite element analysis of steel plate and CFRP laminate strengthened beams. It is seen that shear stress is high at the plate end, reduces exponentially towards the mid-span of strengthening plate and finally becomes constant (Figure 3). Since this high shear stress at the plate end is the key parameter to cause plate end debonding, anchoring using L-shape plates in this zone could be sufficient. End anchors of 100 mm were therefore chosen which allowed some factor of safety. Before placing the end anchors, sikadur adhesive was applied on the prepared bonding face of the beams and the inner face of the anchors. The anchor-plates were then fixed on to the beams and pressed by a rubber roller. After fixing, they were clamped for 3 days for setting.

Materials

Ordinary Portland Cement (OPC) was used in casting the beams and the maximum size of coarse aggregate was 20 mm. The concrete mix was designed for 30 MPa strength. The compressive strength of the concrete was obtained from three cubes after 28 days curing according to British Standard (BS 1881). The measured yield and tensile strength of the stirrups were 520 MPa and 572 MPa respectively. The modulus of elasticity of all steel bars was 200 GPa. For beam strengthening, mild steel plates and CFRP laminates (Sika CarboDur S812) were used. The material properties of main bar, steel plate and CFRP laminate are shown in Table 2.

Instrumentation and test procedure

Figure 4 shows the location of the different instruments used to

Table 1. Test specimens.

Specimen	Designation	Strengthening material			End anchors	
		Type	Thickness (mm)	Width (mm)	Materials	Anchorage length (mm)
1	A1					
2	B0	Steel Plate	2.73	73	-	-
3	B1	Steel Plate	2.73	73	Steel plate	100
4	B2	Steel Plate	2.73	73	Steel plate	200
5	C0	CFRP	1.2	80	-	-
6	C1	CFRP	1.2	80	Steel plate	100
7	C2	CFRP	1.2	80	Steel plate	200

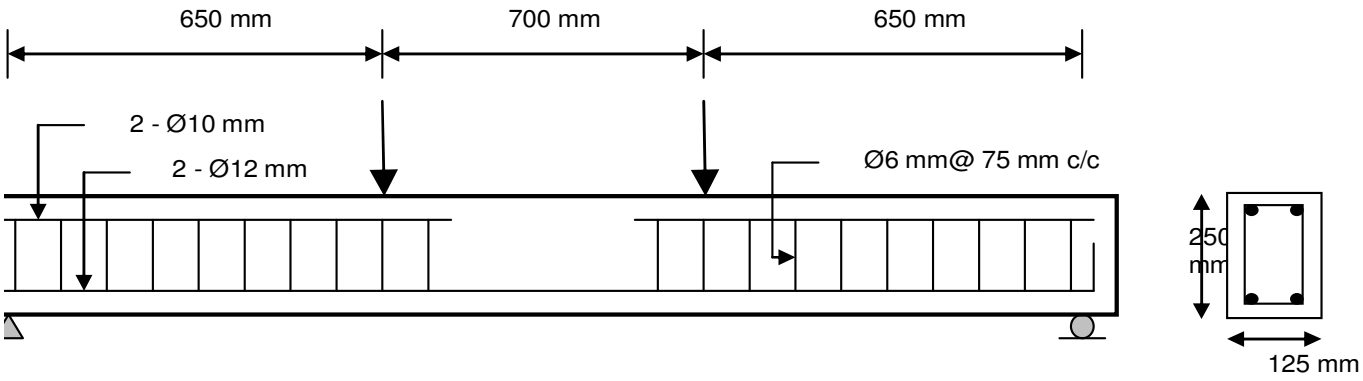

Figure 1. Beam details

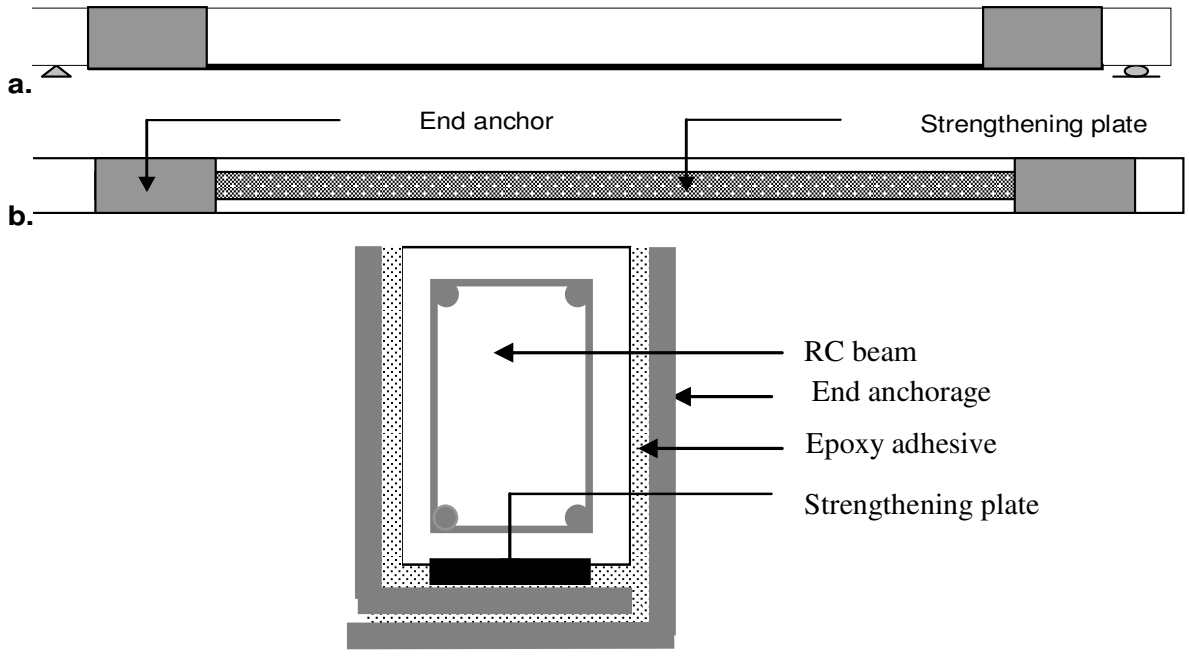

(c) L-shape end anchor

Figure 2. Strengthening and anchoring details. (a) Front view showing the positions of the end anchors. (b) View from the bottom of the r. c. beams showing the end anchors and strengthening plate. (c) L-shape end anchor.

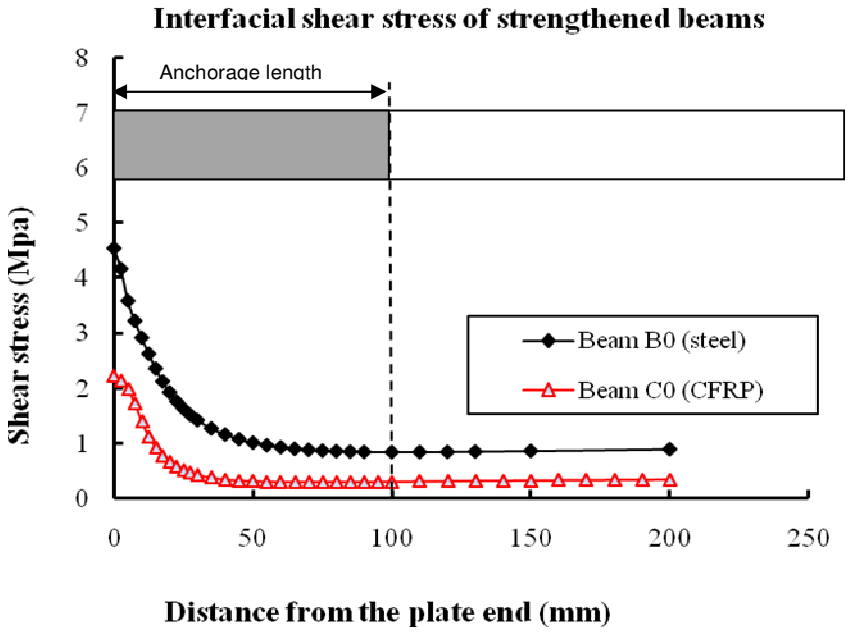

Figure 3. Interfacial shear stress of strengthened beams

Table 2. Material's properties of concrete beams for numerical modelling.

Specimens	Concrete			Steel bar			Strengthening plate		
	f_{cu} (N/mm^2)	E_c (GPa)	Poisson ratio	f_{ys} (N/mm^2)	E_s (GPa)	Poisson ratio	f_{yp} (N/mm^2)	E_p (GPa)	Poison ratio
A1	41.63	30.5	0.2	551	200	0.3			
B1	44.1	31	0.2	551	200	0.3	320	180	0.3
B2	40.89	30	0.2	551	200	0.3	320	180	0.3
C1	40.72	30	0.2	551	200	0.3		165	
C2	36.81	28.5	0.2	551	200	0.3		165	

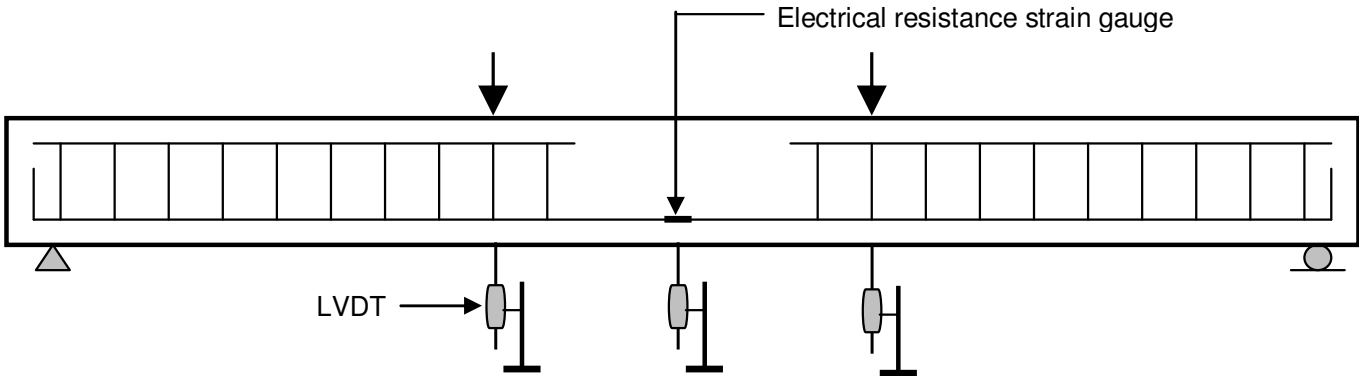

Figure 4. Beam instrumentations.

record data during testing. Electrical resistance strain gauges measured the strains in the steel plate, CFRP laminate and concrete. The demac gauges were also attached along the height of beam at the mid span region to measure the horizontal strains. Three linear variable displacement transformers (LVDTs) were used to measure the vertical deflection of the beam at mid-span and under the two load points (Figure 4). The load was applied incrementally under load control procedures up to failure using the

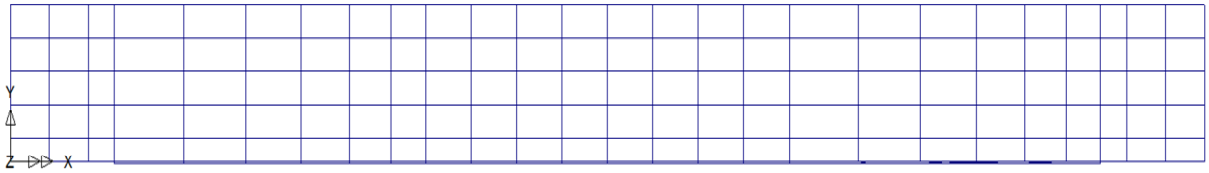

Figure 5. Modelling of strengthened beam.

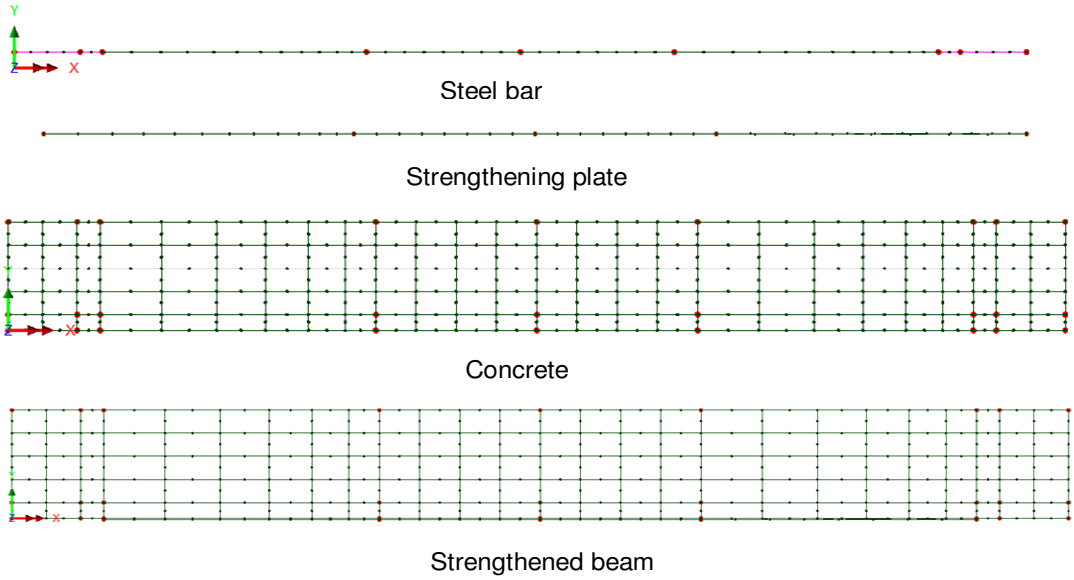

Figure 6. Meshing of strengthened beam.

Instron 8505 Universal testing machine.

FINITE ELEMENT METHOD (FEM) ANALYSIS

Discretization

In the numerical analysis, a finite element program (LUSAS) is used to investigate the structural behaviour of end anchored steel plate and CFRP laminate flexurally strengthened r. c. beams. 2-D surface elements are used to model the concrete beams and strengthening plates. Line elements are used to model the reinforcing bars. The steel plate and CFRP laminate surface elements are attached to the bottom surface of the concrete beam directly (Figure 5). Perfect bonding between strengthening plate and the concrete surface is assumed to avoid premature debonding failure (Li et al., 2006).

Meshing

Reinforcing bars were meshed using a line mesh with two dimensional structural bar elements. Concrete and strengthening plates were meshed using quadrilateral plane stress elements. In all cases, quadratic interpolation was used. Two different mesh divisions were chosen to model the beams. Between the two load points, a regular mesh with four divisions was used. However, from the ends of the beam to the load point, six divisions with uniform transition ratio of first to last element two is used. The detailed of mesh is shown in Figure 6.

Model of concrete beams

A multi crack concrete model is used to model the concrete beam. The difficulties relating to concrete material modelling are various and manifold; these include: increasing deviatoric strength with increasing triaxial confinement, non-linear behaviour in compression, loss of tensile strength with compressive crushing, softening in tension leading to the formation of fully formed stress-free cracks, aggregate interlock on partially and fully formed cracks, and crack opening and closing with both shear and normal crack surface movements. The model uses a fully implicit approach and unlike most plastic damage models does not use scalar damage variables but instead requires the computation of the derivative of the principal stress and projection tensors with respect to the Cartesian stress components. In this respect, the plastic-damage model is perhaps the most relevant to the one implemented here. Table 2 gives materials constants for the concrete beams.

Models of steel bar

The steel bars are modelled using 2-node bar elements that can only transmit longitudinal force where the nodal variables are only U and V (Figure 7). The element strain-displacement relationship and thermal strain vector are defined in the local Cartesian system as:

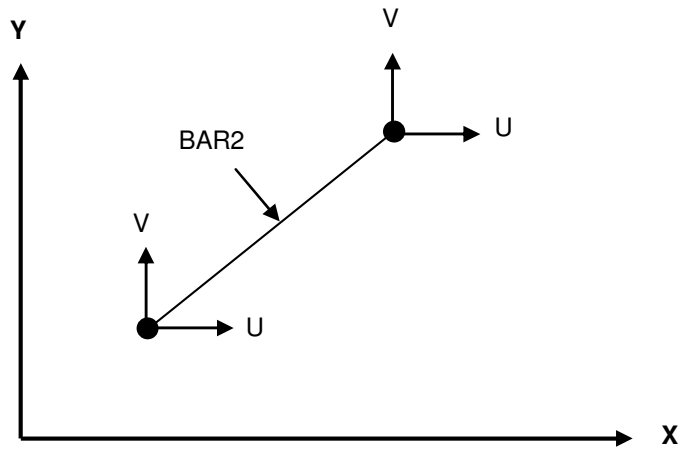

Figure 7. Nodal Freedoms for 2-D BAR Elements.

$$\epsilon_x = \frac{\partial U}{\partial X}$$

$$(\varepsilon_0)_T = \alpha T \quad (1)$$

And the elastic constitutive relationship is defined as:

$$\sigma_x = E\epsilon_x \quad (2)$$

Models of steel plate and CFRP laminate

The steel plate is considered as an isotropic elasto-plastic material whereas CFRP laminates are considered anisotropic elastic material. All these materials are modelled using the von Mises stress potential model. The von Mises criterion is the most universally accepted yield criterion for metals. The criterion is based on considerations of distortional strain energy. The plane stress elements are formulated by assuming that the variation of out of plane direct stress and shear stresses is zero. Thus, the infinitesimal strain-displacement relationships are defined as:

$$\epsilon_X = \frac{\partial U}{\partial X}$$

$$\epsilon_Y = \frac{\partial V}{\partial Y}$$

$$\gamma_{XY} = \frac{\partial U}{\partial X} + \frac{\partial V}{\partial Y}$$

The isotropic elastic modulus matrices is:

$$D = \frac{E}{(1-v^2)}\begin{bmatrix} 1 & v & 0 \\ v & 1 & 0 \\ 0 & 0 & \frac{1-v}{2} \end{bmatrix} \quad (3)$$

Where; E is Young's modulus, V is Poisson's ratio and D is the Material modulus matrix.

Method of analysis

The beams were analyzed using the nonlinear and transient option of the package. The automatic nonlinear incrementation option was selected. A maximum of twenty five iterations was used. Termination criteria were selected based on maximum deflection at mid-span. The boundary conditions of the beams were chosen as fixed in vertical direction (Y). Translation in X and Z direction and rotation in all three directions are free. Point loads were used for analysis.

TEST RESULTS

Mode of failure

Figure 8 shows the results obtained from beams specimens at failure. The control beam (A1) showed a flexural and ductile mode of failure. The un-anchored steel plate (B0) and CFRP laminate (C0) strengthened beams failed by plate end interfacial debonding and concrete cover separation failure respectively. However, end anchored steel plate strengthened beams (B1 and B2) and CFRP laminate strengthened beams (C1 and C2) failed by flexure and shear respectively rather than by premature plate end debonding.

In the case of un-anchored strengthened beams (B0 and C0), the debonding failure was initiated because of the formation of shear cracks at the plate ends. The mechanism of debonding failure can be attributed to the discontinuity at the plate end, whereby excessive shear and normal stresses would normally develop. El-Mihilmy and Tedesco (2001) reported that when this shear stress exceeds the shear resisting capacity of the concrete, shear cracks occur at the end of the plate. This results in the plate being debonded either at the level of internal reinforcement or at the bonding interface. L-shaped end

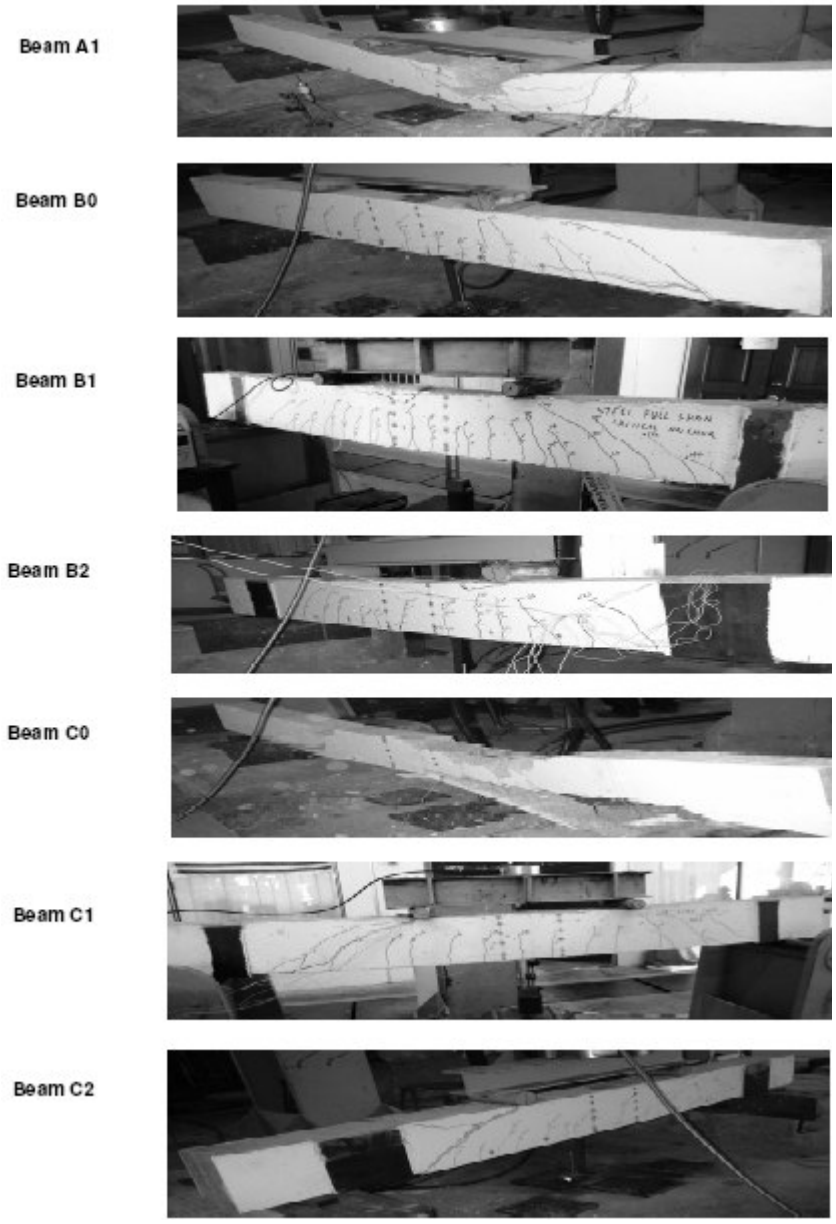

Figure 8. Failure mode of tested specimens.

anchors significantly reduce these shear cracks (Jumaat and Alam, 2008; Bahn et al., 2008). Because of their shapes, inner sides of the plates can be attached firmly to the sides of the beams, which increases the shear strength in that portion of the beams. As the shear strength increases, the risk to form shear cracks at the ends of the plate is reduced. Thus plate debonding does not occur.

In this research, a minimum anchorage length (100 mm) of end anchors was used for beams B1 and C1. This minimum anchorage length was obtained from the interfacial shear stress diagram as shown in Figure 3. The results showed that the optimized end anchored strengthened beams (B1 and C1) did not fail by plate end debonding and had an identical failure behavior with the arbitrarily anchored strengthened beams (B2 and C2). This indicates that optimized end anchors provide sufficient anchorage which covered the high interfacial shear stress of strengthened beams (Figure 3). Since the high shear stress zone was covered by end anchors, plates did not debond from the end until the beams failed by flexure or shear. Thus, beams B1 and C1 showed identical behaviour with their corresponding arbitrarily anchored strengthened beams (B2 and C2 respectively).

Results also showed that the un-anchored CFRP laminate strengthened beams failed by concrete cover

Table 3. Experimental result.

Specimen	Experimental results							
	1st Crack load (kN)	Increase over Control Beam (%)	Ultimate load (kN)	Increase over control beam (%)	Deflection at yield (1)	Deflection at failure (2)	Ductility factor (2/1)	Mode of failure
A1	12		83		7.58	18.58	2.45	Flexure
B0	35	190	104.3	25	-	7.8	0	Debonding
B1	30	150	137	65	9.1	33.1	3.64	Flexure
B2	35	190	130.9	58	12.18	28.96	2.38	Flexure
C0	27	125	123.9	49	-	10.7	0	Debonding
C1	25	108	148	78	10.4	19.4	1.87	Shear
C2	27	125	145.8	76	10.73	23.54	2.19	Shear

delamination whereas the steel plate strengthened beams failed by plate end interfacial debonding. The failure modes of un-anchored CFRP laminate and steel plate strengthened beams were different because of the difference of shear and normal stress intensity at the plate end. A stiffer and thicker plate causes higher shear and normal stresses at the plate end. High shear and normal stresses cause the plates to debond earlier from bonding interface rather than the level of internal reinforcement. This type of failure is called plate end interfacial debonding. In this study, the steel plate had a higher thickness and stiffness than the CFRP laminate. Hence it was expected that the steel plate strengthened beam (B0) failed earlier than CFRP laminate strengthened beam (C0) even though both beams were designed for the same strength. However, due to the delay of laminate debonding, the resultant debonding mechanism of CFRP laminate strengthened beam was found to be more explosive than that of the steel plate strengthened beam. Furthermore, end anchored CFRP laminate strengthened beams failed by premature shear, whereas steel plate strengthened beams failed by flexure followed by crushing of concrete. This difference is thought to be due to the high strength and linear elastic behaviour of CFRP laminate.

Failure load

A summary of the experimental results is presented in Table 3. The test results showed that all un-anchored and end anchored strengthened beams had higher failure loads than the control beam. It is seen that the ultimate loads of end anchored steel plate and CFRP laminate strengthened beams (B1, B2, C1 and C2) were higher than the ultimate loads of the beams without end anchors (B0 and C0). This was because of the presence of end anchors that prevented premature plate end debonding. In the case of strengthened beams without end anchors, premature plate end debonding occurred. However, end anchored strengthened beams attained the full strength before failure which enhanced the ultimate strength over un-anchored strengthened beams. Results also showed that the failure loads of beams B1 and B2 were almost the same. The similar behavior was also found in the case of beams C1 and C2. The end anchored CFRP laminate strengthened beams carried more load than the steel plate strengthened beams. This could happen due to the linear elastic behaviour of CFRP laminate until failure of the beams. Thus, CFRP laminate strengthened beams could carry more loads after the yielding of the bars. In the case of steel plate strengthened beams, the steel plates yielded before yielding of the internal bars. As a result, beams failed immediately after yielding of the internal bars.

Ductility

The load-deflection curves for the beams are shown in Figure 9. All the beam specimens display linear elastic behaviour at the beginning. There was no noticeable difference in deflection of end anchored and un-anchored strengthened beams in the elastic region. However, before failure, the end anchored strengthened beams showed more deflection than the un-anchored strengthened beams. The reason is that end anchors prevent premature failure of the beams and enhance the internal steel bars to yield (Figure 12), thus beams could deflect more at the failure stage. The displacement ductility factor is defined as the ratio of mid-span deflection at failure to midspan deflection at steel bar yield (Bahn and Harichandran, 2008). The ductility factors of all the beams are shown in Table 3. The ductility factors of end anchored strengthened beams were higher than un-anchored strengthened beams because end anchors prevented premature plate end debonding failure and it enhanced to fail the beams in conventional failure mode by yielding of steel bar. Thus, the end anchored strengthened beams showed more displacement before failure. The ductility factor of optimized and arbitrary end anchored strengthened beams were almost identical.

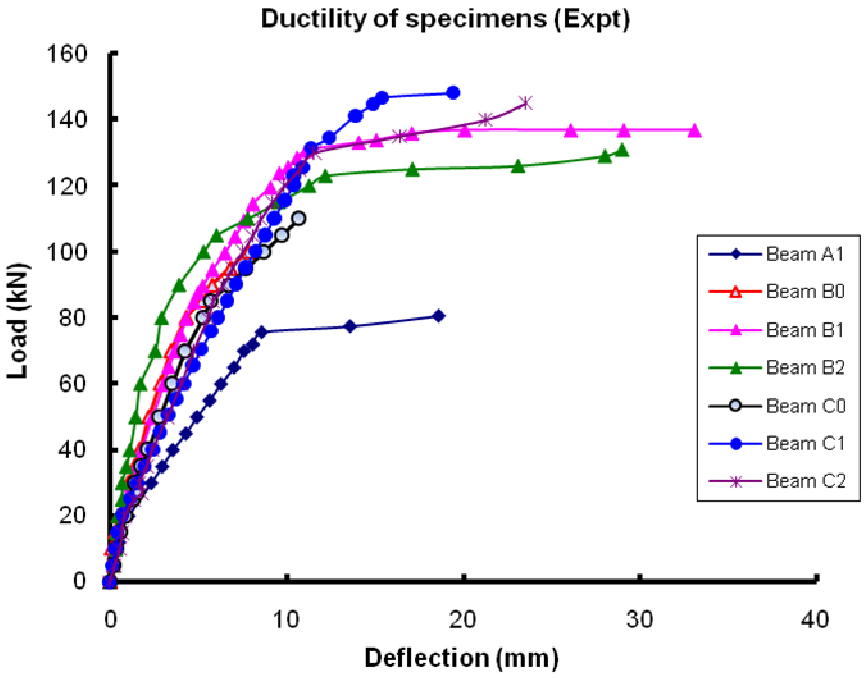

Figure 9. Ductility of beam specimens.

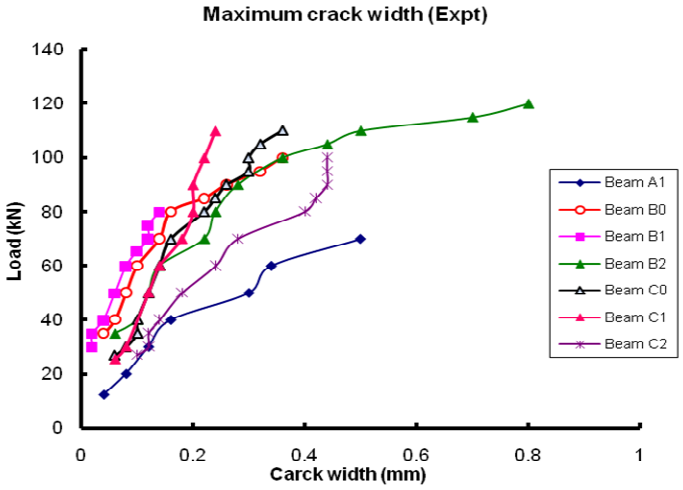

Figure 10. Maximum crack width of beam specimens

Cracking patterns

The first crack loads are shown in Table 3. The strengthened beams in general showed higher cracking loads than the control beam. Since first crack load depends on the modulus of rupture of the concrete and the stiffness of strengthening materials, the first crack loads of both the un-anchored and end anchored steel plate strengthened beams were found to be similar. The same was also noted on the CFRP laminate strengthened beams. Further, optimized and arbitrary end anchored strengthened beams were found to display similar cracking patterns. However, because of the higher stiffness of steel plate, steel plate strengthened beams gave a higher cracking load compared to CFRP laminate strengthened beam. Figure 10 shows the load versus crack width of all the beams. The crack widths of first crack of beams were measured at the level of internal reinforcement. The strengthened beams showed smaller crack widths compared to the control beam. It is also seen that, steel plate strengthened beams showed a smaller crack width compared to CFRP laminate

Table 4. Comparison of experimental results with numerical analysis (end anchored strengthened beams).

Specimen	Cracking load (kN)		Bar yield load (kN)		Plate yield load (kN)		Failure load (kN)		Mode of failure	
	Expt.	FEM	Expt.	FEM	Expt.	FEM	Expt.	FEM	Expt.	FEM
A1	12	12	70	72			83	75	Flexure	Flexure
B1	30	26	120	133	85	102	137	137	Flexure	Flexure
B2	35	22	123	126	90	94	130.9	130	Flexure	Flexure
C1	25	22	122.9	130			148	170	Shear	Flexure
C2	27	22	125	125			145.8	137	Shear	Flexure

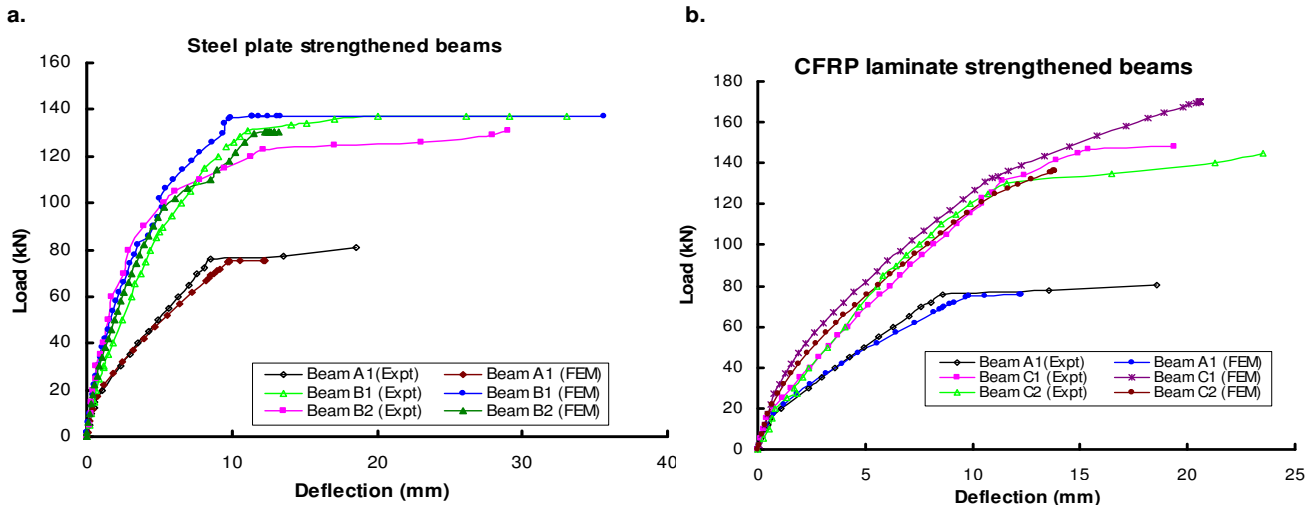

Figure 11. (a): Load vs. deflection (end anchored steel plate strengthened beams). (b). Load vs. deflection (end anchored CFRP laminate strengthened beams).

strengthened beams.

COMPARISON OF TEST AND NUMERICAL RESULTS OF END ANCHORED STRENGTHENED BEAMS

Mode of failure, crack load, yield load and ultimate load

The experimental and numerical failure mode, cracking load, bar yield load and failure loads recorded by all the beams are shown in Table 4. The results showed that the failure mode of beams A1, B1 and B2 obtained from numerical results were similar to the experimental results. It is also noticed that the cracking loads, yield loads and ultimate loads of all beams based on numerical results are identical with the experimental results.

Deflection

The load-mid span deflection curves based on experimental and numerical results for beams A1, B1, B2, C1 and C2 are shown in Figures 11a and b. It is seen that both results show the similar behaviour of deflections for all the beams. All the beam specimens display linear elastic behaviour at the beginning followed by a first crack within the constant moment region of the beam. Thereafter, the load deflection curve becomes highly nonlinear as numerous flexural cracks develop and the beam deflection increases considerably. All the strengthened beams showed smaller deflection than the control beam due to their higher stiffness. Figures 11 (a, b) also show that the deflection of beams A1, B1, B2, C1 and C2 suddenly increased after around 70, 120, 123, 123 and 125 kN load respectively. This was due to steel bar yielding. When the bar was yielding, the strain of the bar increased suddenly allowing greater beam deflection. The result also showed that there was no noticeable difference in deflection of 100 and 200 mm end anchored strengthened beams in the elastic region.

Strains characteristics

The experimental and numerical steel bar strains of all the beams are shown in Figures 12a and b. It is seen in

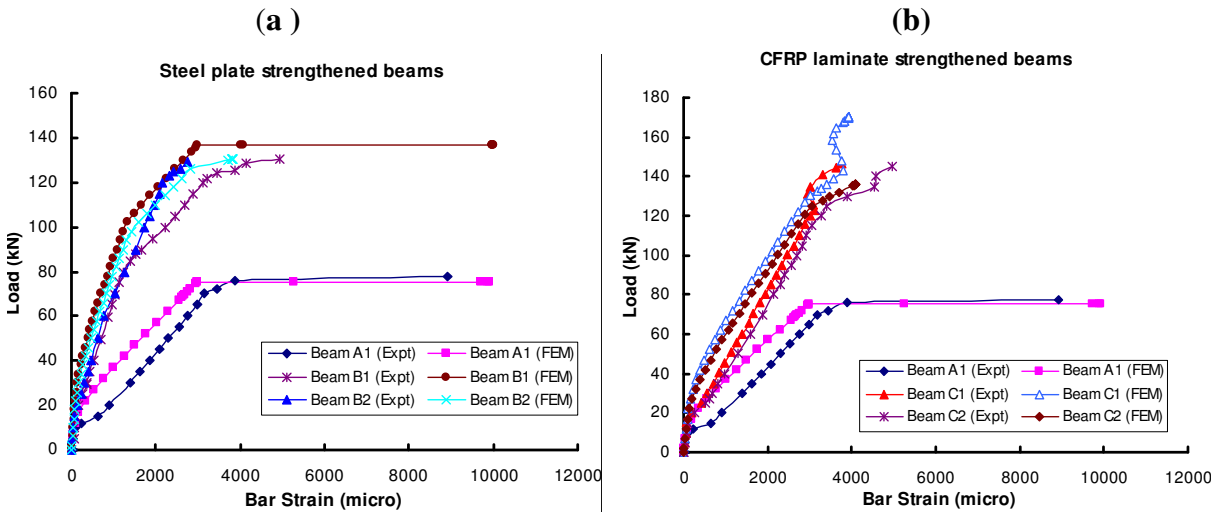

Figure 12. (a): Load vs. bar strain (end anchored steel plate strengthened beams). (b): Load vs. bar strain (end anchored CFRP laminate strengthened beams).

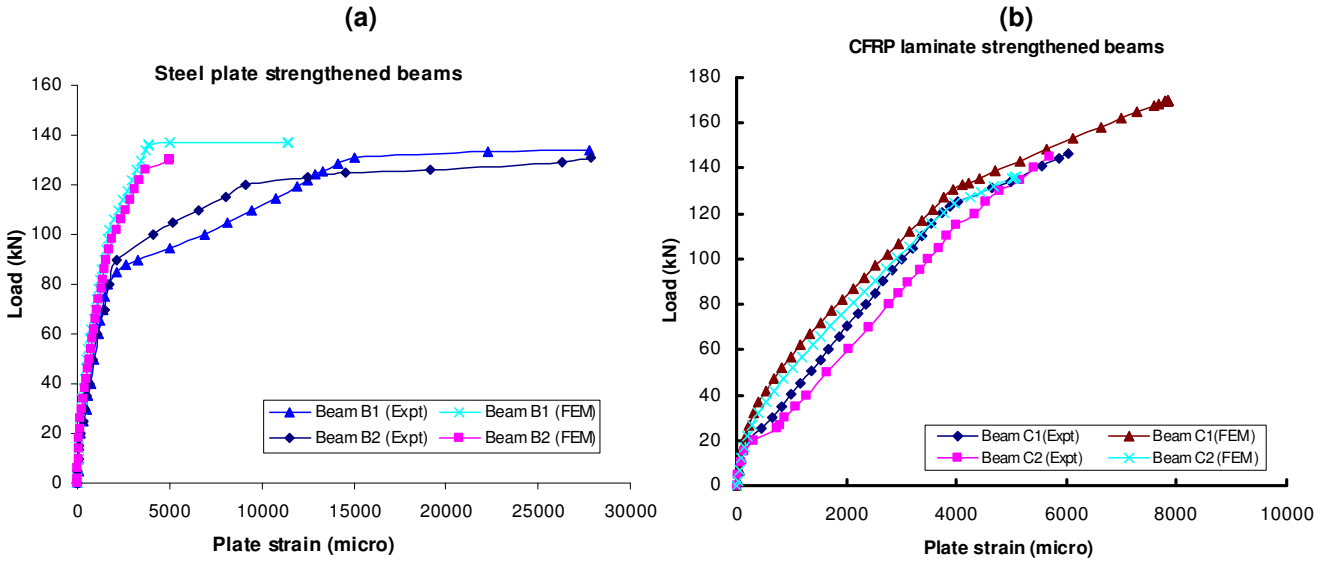

Figure 13. (a): Load vs. Plate strain (end anchored steel plate strengthened beams). (b): Load vs. plate strain (end anchored CFRP laminate strengthened beams).

the figures that bar strains from numerical modelling are close to the experimental value. However, due to the higher stiffness of the strengthened beams, at all load levels, the bar strains of strengthened beams were found to be less than the control beam. Figure 12a shows that the bar strain of the steel plate strengthened beams (B1 and B2) was identical due to the similar material properties of both of the beams. This was also true for CFRP laminate strengthened beams. The approximate bar yield loads of all the beams are shown in Table 4. Figures 13a and b represents the plate strain of all strengthened beams based on experiment and numerical model. The figures show that plate strain from both results were identical.

The numerical results of concrete compressive strain for all the beams are identical with the experimental results (Figures 14a and b). From the Figures 14 a and b, it is seen that at any load, all strengthened beams showed less concrete strain than the control beam. For all beams, the concrete compressive strain was less than 0.0035. Figures 14a and b also show that before failure, end anchored strengthened beams had shown higher concrete compressive strain than the control beam. Since end anchored strengthened beams had shown higher

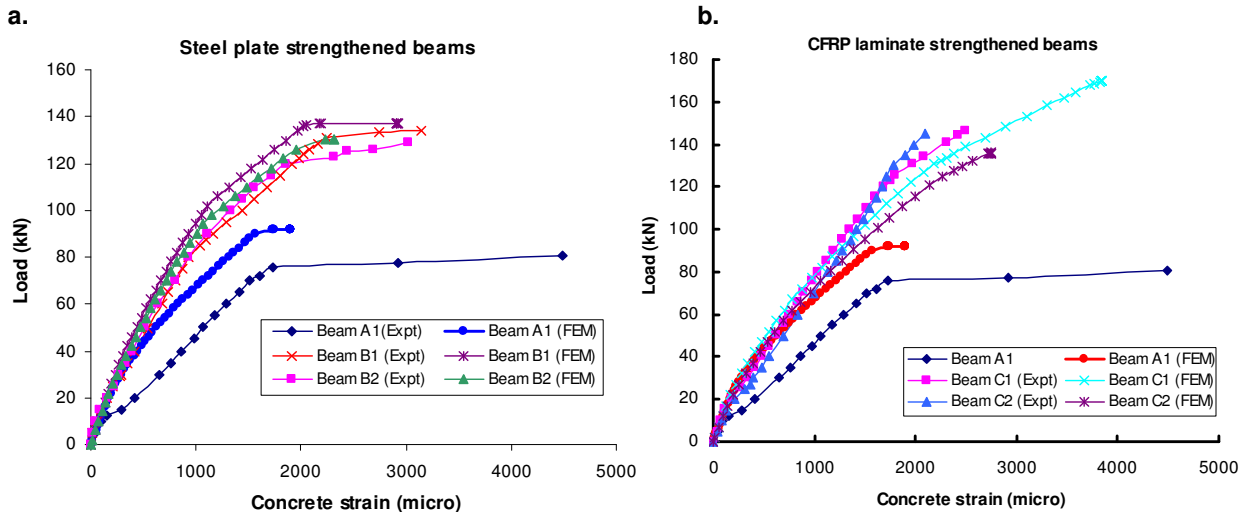

Figure 14. (a): Load vs. Concrete strain (end anchored steel plate strengthened beams). (b): Load vs. Concrete strain (end anchored CFRP laminate strengthened beams).

failure loads than the control beam, these beams showed higher concrete compressive strain at failure. Furthermore, the concrete compressive strain of end anchored steel plate strengthened beams suddenly increased at about 120 kN load. This is due to the yielding of the steel bar. After bar yielding, the bar strain increased rapidly, thus the concrete strain would also increase due to strain compatibility which is the sign of flexural failure followed by crushing of concrete.

Conclusion

The conclusions from the present study can be summarized as follows:

1. All end anchored strengthened beams showed higher failure loads compared to their corresponding un-anchored strengthened beams. The optimized end anchored strengthened beams had shown similar failure loads to arbitrarily end anchored strengthened beams. All strengthened beams gave higher failure loads than the control beam.
2. End anchored CFRP laminate strengthened beams gave higher failure loads compared to steel plate strengthened beams.
3. Un-anchored steel plate and CFRP laminate strengthened beams failed by plate end debonding and concrete cover separation failure respectively. For both the optimized and arbitrarily end anchor plates, the failure modes were found to be similar. Optimized end anchored steel plate and CFRP laminate strengthened beams failed in flexure and shear respectively. All end anchored strengthened beams showed ductile mode of failure.
4. The cracking load of the control beam was found to be less than the strengthened beams. The steel plate strengthened beam gave a higher cracking load and smaller crack widths than the CFRP laminate strengthened beam. Un-anchored and end anchored strengthened beams had identical crack loads. Optimized and arbitrarily end anchored strengthened beams had shown similar cracking patterns.
5. The failure loads, cracking loads, deflections and the strain characterises (bar, plate and concrete) of all end anchored strengthened beams based on numerical analysis were found to be similar with the experimental results. Numerical and experimental analysis found that all strengthened beams had less bar, plate and concrete strain than the control beam. The bar yield strains and loads of all end anchored strengthened beams were found to be similar.

ACKNOWLEDGEMENTS

The authors would like to thank the Majlis Penyelidikan Kebangsaan Sains Negera under science fund 13-02-03-3022 for providing the fund to carry out the work reported in this paper. Thanks are also due to Sika Kimia and their staff for providing the technical and materials supports for this work. The authors would also like to express their gratitude to whosoever had contributed to this work either directly or indirectly.

REFERENCES

Bahn BY, Harichandran RS (2008). Flexural behaviour of reinforced concrete beams strengthened with CFRP sheets and epoxy mortar. J. Composites Construction 12(4): 387-395.
Ceroni F, Pece M, Mathys S, Taerwe L (2008). Debonding strength and anchorage devices for reinforced concrete elements strengthened with FRP sheets. Composites: Part B. 39: 429-441.
Chahrour A, Soudki K (2005). Flexural response of reinforced concrete beams strengthened with end-anchored partially bonded carbon

fiber-reinforced polymer strips. J. Composites Construction. 9(2): 170-177.
El-Mihilmy MT, Tedesco JW (2001). Prediction of anchorage failure for reinforced concrete beams strengthened with fiber-reinforced polymer plates. ACI Structural J. 98(3): 301-314.
Garden HN, Hollaway LC (1998). An experimental study of the influence of plate end anchorage of carbon fibre composite plates used to strengthen reinforced concrete beams, Composite Structures 42: 175-188.
Hosny A, Shaheen H, Abdelrahman A, Elafandy T (2006). Performance of reinforced concrete beams strengthened by hybrid FRP laminates. Cement Concrete Composites 28: 906-913.
Hussain M, Sharif A, Basunbul A, Baluch MH, Al-Aulaimani GJ (1995). Flexural behavior of precracked reinforced concrete beams strengthened externally by steel plates. ACI Structural J. 92(1): 14-22.
Jones R, Swamy RN, Charif A (1998). Plate separation and anchorage of reinforced concrete beams strengthened by epoxy-bonded steel plates. Structural Eng. 66(5): 85-94.
Jumaat MZ, Alam MA (2008). Behaviour of U and L shaped end anchored steel plate strengthened reinforced concrete beams. Eur. J. Sci. Res. 22(2): 184-196.
Kim YJ, Wight RG, Green MF (2008). Flexural strengthening of RC beams with prestressed CFRP sheets: using non-metallic anchor systems. J. Composites Construction. 12(1): 44-52.
Li LJ, Guo YC, Liu F, Bungey JH (2006). An experimental and numerical study of the effect of thickness and length of CFRP on performance of repaired reinforced concrete beams. Construction Building Mater. 20: 901-909.
Saadatmanesh H, Malek AM (1998). Design guidelines for flexural strengthening of RC beams with FRP plates. J. Composites Construction ASCE. 2(4): 158-164.
Smith ST, Teng JG (2002). FRP-strengthened RC beams. I: review of debonding strength models. Eng. Structures 24: 385–395.
Yang J, Ye J, Niu Z (2008). Simplified solutions for the stress transfer in concrete bems bonded with FRP plates. Eng. Structures 30: 533-545.
Yao J, Teng JG (2007). Plate end debonding in FRP-plated RC beams-I: Experiments. Eng. Structures 29:: 2457-2471.